NANO LETTERS

2005
Vol. 5, No. 7
1273−1277

Storage of Molecular Hydrogen in B–N Cage: Energetics and Thermal Stability

Qiang Sun,* Qian Wang, and Puru Jena

Physics Department, Virginia Commonwealth University, Richmond, Virginia 23284-2000

Received March 1, 2005

ABSTRACT

Using first principles theory based on density functional formulation we have studied the energetics and thermal stability of storing hydrogen in B–N-based nanostructures. We show that hydrogen molecule enters through the hexagonal face of the $B_{36}N_{36}$ cage and prefers to remain inside the cage in molecular form. The energy barriers for the hydrogen molecule to enter into or escape from the cage are respectively 1.406 eV and 1.516 eV. As the concentration of hydrogen inside the cage increases, the cage expands and the bond length of the hydrogen molecule contracts, resulting in significant energy cost. At zero temperature, up to 18 hydrogen molecules can be stored inside a $B_{36}N_{36}$ cage corresponding to a gravimetric density of 4 wt %. However, molecular dynamics simulation by using Nose algorithm at room temperature (T = 300 K) indicates that high weight percentage hydrogen storage cannot be achieved in B–N cage structures and thus these materials may not be good for practical applications.

Hydrogen storage is considered to be the biggest challenge in a new hydrogen economy because the storage medium must meet the requirements of high gravimetric and volumetric density, fast kinetics, and favorable thermodynamics.[1−7] The current methods of storing hydrogen as compressed gas or in the liquid form do not meet the industry requirements because the energy densities are much lower than that in gasoline. Moreover, there are issues of safety and cost involved in compressing hydrogen under high pressure or liquefying it at cryogenic temperatures. Although storage of hydrogen in solid-state materials offers an alternative, there are no current solid-state storage materials that meet the industry requirements.

Hydrogen can be stored in solid materials either in atomic or molecular form. In metal hydrides, hydrogen molecules dissociate on the metal surface and reside in interstitial positions in atomic form and can diffuse readily. In complex light metal hydrides, on the other hand, hydrogen atoms are held by strong covalent bonds and their dissociation requires high temperatures. Storage of hydrogen in molecular form has an advantage in that molecular hydrogen has fast kinetics. However, their bonding is very weak and desorption can take place at low temperatures. Recently, considerable attention has been focused on porous materials[8−14] such as clathrates, zeolites, carbon nanotubes, and fullerenes as possible materials for hydrogen storage. Early experiments on carbon nanotubes have met with some controversy, and very different results for their hydrogen storage capacity have been reported. Tibbetts and co-workers claimed that any reported capacity of higher than 1 wt % is due to experimental error.[15] Shiraishi and co-workers reported hydrogen gravimetric density of only 0.3 wt %.[16] Kajiura et al.[17] measured the hydrogen storage capacity of five types of commercially available carbon materials with different nanostructures at up to 8 MPa at room temperature. Using an apparatus where the error in the gravimetric density is less than 0.04 wt %, they reported the highest storage capacity to be 0.43 wt %. Recent theoretical study indicates that high hydrogen content in the pure carbon nanotubes cannot be achieved through physical sorption.[18] Doping transition metals can improve the absorption, but the large mass for the metal atoms can reduce the gravimetric density. Furthermore, doping is not easily controlled in the experiment.

Because of these shortcomings of carbon nanotubes, recent efforts have been directed at non-carbon nanosystems composed of light elements such as B and N. B−N nanostructures are an analogue of the carbon ones and offer many advantages. For example, carbon nanotubes are oxidized at 600 °C in air while B−N nanotubes are stable up to 1000 °C. In addition to their heat resistance in air and structural stability, B−N nanotubes are semiconducting with wide band gaps (5.5 eV) that is nearly independent of tube diameter or helicity. With the advancement in synthesis techniques, many novel forms of B−N nanostructures such as nanotubes,[19−26] bamboo-like wires,[27] nanocages, and nanocapsules[28] have been discovered. Furthermore, several authors have also studied the hydrogen uptake and reversibility issues of B−N nanostructures.[26,28−30] It has been found experimentally that at 10 MPa the B−N nanotubes can store as much as 2.6 wt % of hydrogen, while bulk B−N powder

10.1021/nl050385p CCC: $30.25
Published on Web 05/26/2005

can store only 0.2 wt %. This clearly shows that nanostructures provide added advantage in storing hydrogen. Although calculations at the semiempirical level have been performed on the interaction of hydrogen with B−N cages,[29,30] full understanding of this system is lacking. For example: (1) Does hydrogen prefer to reside on the surface of the cage or does it enter into the cage? (2) What is the energy barrier for hydrogen to enter into or escape from the cage? (3) Once hydrogen enters into the cage structure, does it remain in molecular or dissociated state? (4) What is the maximum number of hydrogen molecules that can be stored inside a cage before the cage breaks? (5) As more hydrogen molecules are stored, how are the geometry and electronic structure of the cage changed? (6) What is the effect of temperature on the stability of the hydrogen storage material? In this paper, we provide detailed study for these questions by using $B_{36}N_{36}$ cage as an example.

Spin-polarized calculations of total energies and forces, and optimizations of geometry were carried out using a plane-wave basis set with the projector augmented plane wave (PAW) method[31] as implemented in the Vienna ab initio Simulation Package (VASP).[32] In the PAW approach, charge and spin densities are decomposed into pseudodensities and compensation densities which account for the difference between the pseudodensities and all-electron densities. The pseudodensities consist of a smooth part expressed in a plane-wave representation and localized augmentation charges that account for the violation of norm conservation. The structure optimization is symmetry unrestricted and uses a conjugate-gradient algorithm. The exchange-correlation PW91 functional is used.[33] We have used super-cells with 15 Å vacuum spaces along the *x*, *y*, and *z* directions for all the calculated structures. The Γ point is used to represent the Brillouin zone due to the large supercell. The energy cutoff was set to 400 eV and the convergence in energy and force were 10^{-4} eV and 1×10^{-3} eV/Å, respectively.

The accuracy of our computational method was tested by computing the binding energy and bond length of H_2 as well as the geometry and binding energy of the $B_{36}N_{36}$ cage. The calculated bond length and binding energy of H_2 are 0.749 Å and 4.536 eV, respectively, which are in good agreement with the experimental values of 0.741 Å and 4.533 eV.[34] For the $B_{36}N_{36}$ cage, there are 36 BN pairs distributed in 6 four-membered rings and 32 six-membered rings. The optimized structure is found to have T_d symmetry. The average binding energy per atom and the highest occupied and lowest unoccupied (HOMO−LUMO) energy gap are 8.48 and 5.35 eV, respectively. The average B−N bond length is 1.465 Å, and the average cage radius is 3.940 Å. In the four-membered rings, the average length of the B−N bond is 1.468 Å, the average B−N−B angle is 77.59 degrees and the average N−B−N angle is 99.90 degrees. The results agree well with previous ab initio calculations.[35]

We first discuss the interaction of a single H_2 molecule with the $B_{36}N_{36}$ cage and determine if it binds associatetively or dissociatively and if it remains on the outer surface of the cage or inside? In the latter case, we are interested in knowing how it enters into the cage: through the square or the hexagonal face. To find answers to these questions we have studied three different configurations. In configuration I, H_2 was located on the top of the B or N site on the cage surface (see top panel in Figure 1a). It is found that H_2 can weakly bind on N sites with the physisorption energy of 0.11 eV. In the second configuration, we placed H_2 initially in the hollow site of a four-membered ring with one hydrogen atom inside the cage and the other outside the cage (see top panel in Figure 1b). After the structure optimization, we found that the four-membered ring is broken (see bottom panel in Figure 1b), indicating that the four-membered ring is too small for H_2 to go through.

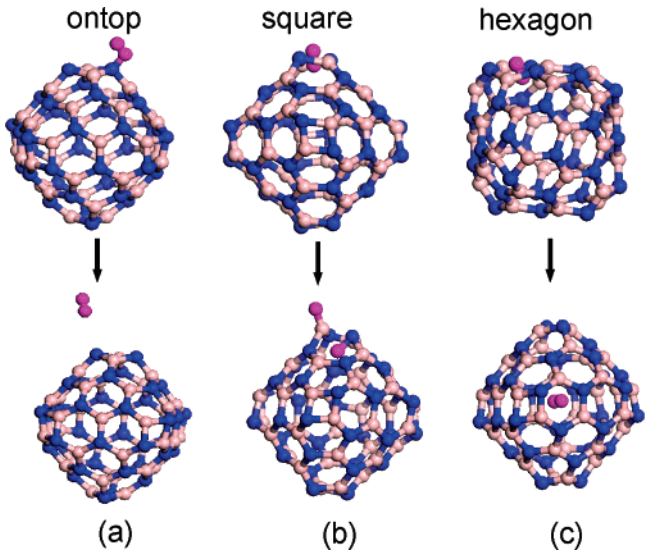

Figure 1. Starting and optimized structures of H_2 interacting with the BN cage.

Table 1. Bond Lengths for B−N (R_1) and H−H (R_2), Symmetry, HOMO−LUMO Gap and Formation Energy (ϵ)

cluster	R_1 (Å)	R_2 (Å)	symmetry	gap (eV)	ϵ (eV)
$B_{36}N_{36}$	1.465		T_d	5.35	
$18H_2@B_{36}N_{36}$	1.504	0.737	C_1	3.69	+35.583
$8H_2@B_{36}N_{36}$	1.474	0.739	C_1	4.60	+7.11
$7H_2@B_{36}N_{36}$	1.472	0.741	C_1	4.77	+5.021
$6H_2@B_{36}N_{36}$	1.469	0.743	C_1	4.88	+2.855
$4H_2@B_{36}N_{36}$	1.468	0.744	D_2	4.90	+1.672
$3H_2@B_{36}N_{36}$	1.467	0.746	C_1	4.91	+0.87
$2H_2@B_{36}N_{36}$	1.466	0.747	D_{2d}	4.95	+0.306
$1H_2@B_{36}N_{36}$	1.465	0.749	D_{2d}	4.88	0.0

The situation is different for the third configuration where H_2 is placed in the hollow site of a six-membered ring (see top panel in Figure 1c). Here we found that the H_2 molecule can go through the six-memberd ring from the outside. Using elastic band method,[36] the energy barrier is found to be 1.406 eV for H_2 insertion through the six-membered ring. This insertion barrier is about 0.4 eV less than the value for H_2 insertion in C_{60} cage.[37] On the other hand, the energy barrier for H_2 to escape from the cage is 1.516 eV, which is 0.24 eV less than the value for H_2 escaping from the C_{60} cage.[37] The main reason for these differences in the energy barriers between B−N and C_{60} cage is that the size of the six-membered ring in $B_{36}N_{36}$ cage is about 5.6% larger than the

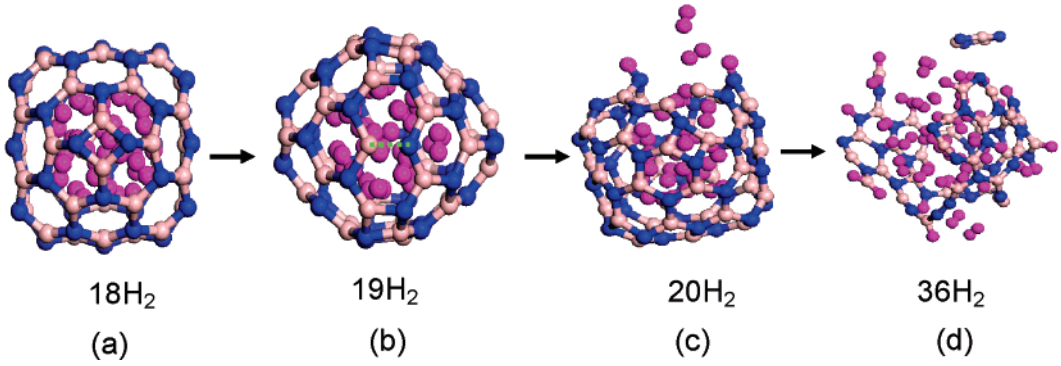

Figure 2. Stability of the cage structure as more H_2 molecules are embedded inside the cage.

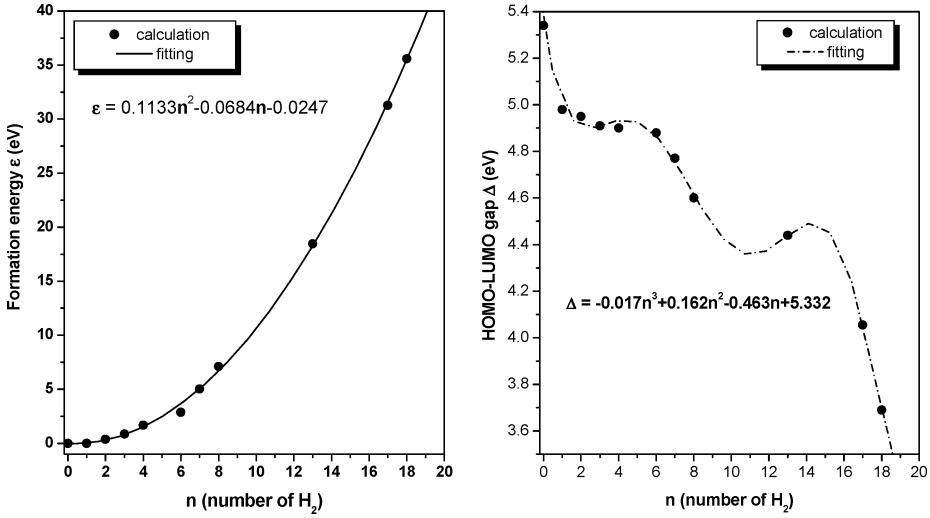

Figure 3. Formation energy and HOMO−LUMO gap as a function of the number of H_2 stored.

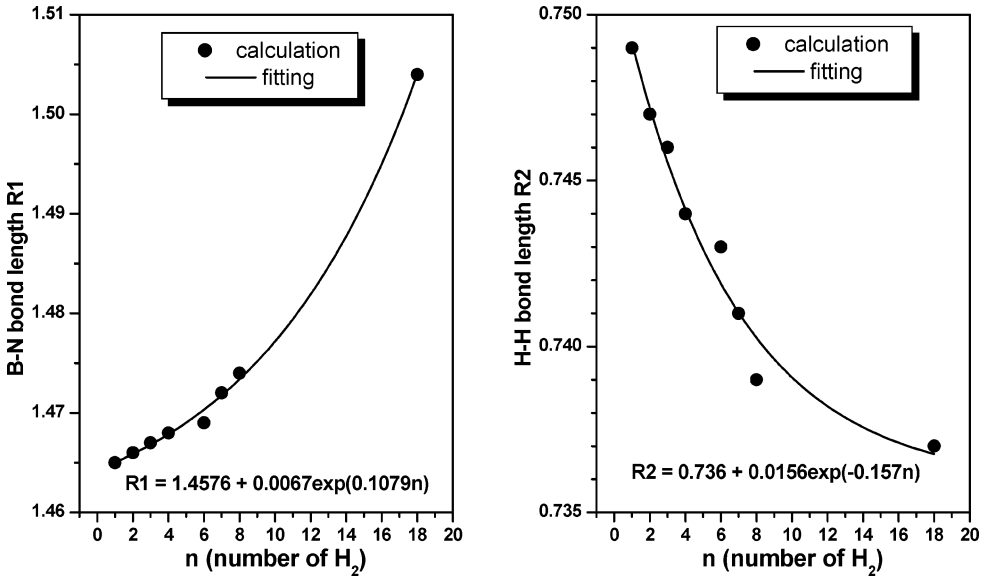

Figure 4. Bond length as a function of the number of H_2 stored.

corresponding size in the C_{60} cage. In the equilibrium configuration, the encapsulated H_2 resides at the center of the cage, resulting in D_{2d} symmetry for the complex (see bottom panel in Figure 1c). It is interesting to note that the formation energy, which is defined as the energy difference between $H_2@B_{36}N_{36}$ and the separated $B_{36}N_{36}$ and H_2, is 0.0 eV within the accuracy of our calculation. This is because there is no change in the bond lengths in both the H_2 molecule and the cage, suggesting that the cavity in $B_{36}N_{36}$ cage is too big for any interaction between the H_2 molecule and the cage. However, when the second H_2 is stored, the formation energy increases to +0.306 eV, as the cage

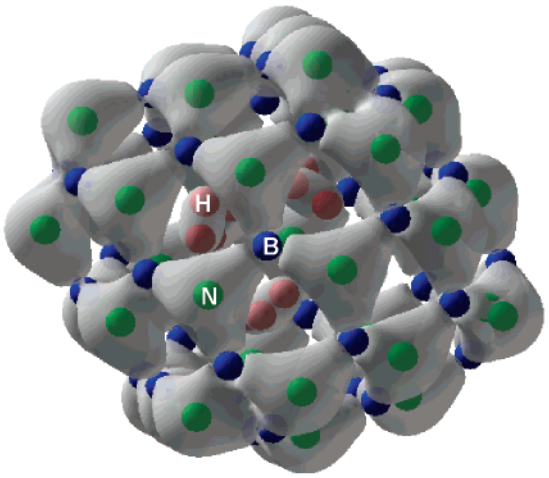

Figure 5. Charge density distribution of $(H_2)_6@B_{36}N_{36}$.

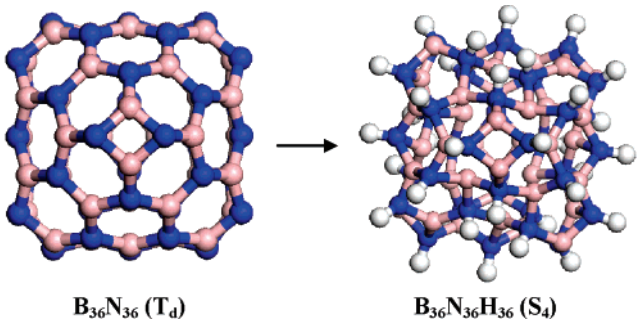

Figure 6. The geometry of $B_{36}N_{36}$ before and after chemisorption of atomic H.

expands while the bond length of H_2 shrinks. This tendency keeps on going up to $n = 18$ H_2 molecules. The B−N bond length increases to 1.504 Å and the H_2 bond decreases to 0.737 Å. This amounts to about 2.7% expansion in BN bond length and 1.6% contraction in the H_2 bond length.

In Table 1 we present the calculated energy costs in storing H_2 molecules. When the number of H_2 molecules increases to 19, one of the bonds in the cage is broken, but all the H_2 molecules still remain inside the cage. When another H_2 is embedded, five B−N bonds break and two H_2 molecules fly out of the cage. When the number of H_2 increases to 36, the B−N cage is totally broken. This process is depicted in Figure 2. Our results indicate that the maximum number of hydrogen stored in $B_{36}N_6$ cage is 18, which corresponds to a gravimetric density of 4 wt %.

In Figure 3 we show the changes in the formation energy and HOMO−LUMO gap as a function of the number (n) of H_2 molecules stored in the cage. The corresponding changes in bond length are given in Figure 4. We see that storage of H_2 in B−N cage costs energy. The required energy increases as n^2, while the HOMO−LUMO gap decreases as n^3. The B−N bond length increases exponentially with n, while the H−H bond length decreases exponentially with n. When the change in bond length exceeds a critical limit, the cage breaks and H_2 molecules are released from the cage. This is shown in Figure 2.

The bonding features of the complex can be seen from the charge density distribution in $(H_2)_6@B_{36}N_{36}$ plotted in Figure 5. Due to the large difference in the electronegativity between B and N, the bonding in the B−N cage is ionic. However, the bonding between H atoms remains covalent due to the shrinking of the hydrogen molecular bond. When the cage breaks, some of the H_2 molecules dissociate and

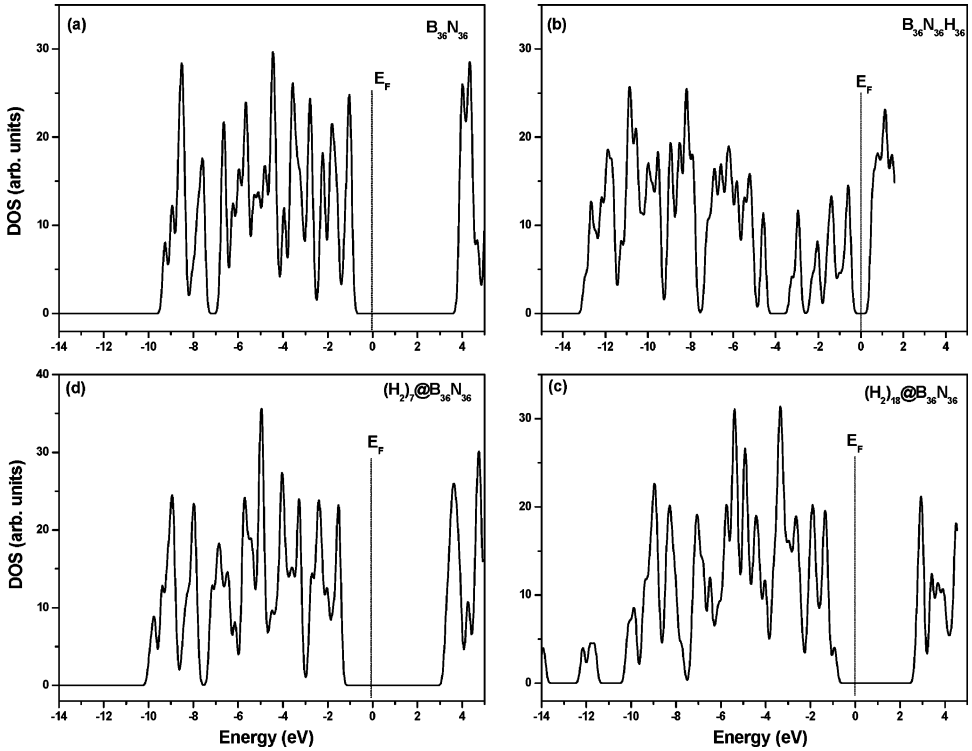

Figure 7. Density of states (DOS) for different configurations of the cage.

bind to the cage while others fly away as molecular hydrogen (see Figures 2c and 2d).

We have also examined the structure of the cage when H binds atomically to the outer surface of the cage, even though this is energetically not favorable. We find that H prefers to bind to the N sites. The cage structure of 36 H atoms bound to 36 N sites on the surface remains even after full relaxation of the geometry, suggesting that this is a metastable state. However, we note that hydrogenation distorts the cage from its initial T_d symmetry to S_4 symmetry, as shown in Figure 6. The average B−N bond length is increased by 7.1% from 1.465 to 1.569 Å. The average N−H bond length is 1.04 Å.

In Figure 7 we plot the density of states (DOS), which shows the changes in electronic structure as molecular and atomic hydrogen are absorbed. The HOMO−LUMO gap of the $B_{36}N_{36}$ cage with 36 H stored molecularly inside the cage is 3.69 eV, which is much larger than the 1.06 eV gap when hydrogen is adsorbed atomically. Consequently, the former is chemically more stable. Indeed the formation energies of atomically and molecularly stored hydrogen $B_{36}N_{36}$ cages are +56.30 and +35.58 eV, respectively.

The large energy cost in storing hydrogen inside the $B_{36}N_{36}$ cage raises an important question: Are these materials suitable for practical applications? In particular, do these materials have thermal stability? To address this question, we have carried out molecular dynamics simulation by using Nose algorithm[38] at finite temperatures. First, we studied the thermal stability of $(H_2)_{18}@B_{36}N_{36}$ structure at room temperature ($T = 300$ K) using molecular dynamics simulation with 0.4 fs time steps. After 0.4 ps simulation, we found that four H_2 molecules escaped out of the $B_{36}N_{36}$ cage. We then reduced the number of H_2 molecules from 18 to 13 and repeated the calculations. However, after 1.3 ps of simulation, three H_2 molecules were found to escape from the BN cage. This indicates that the $B_{36}N_{36}$ cage is not suitable as a practical hydrogen storage material at room temperature.

In summary, we have studied the energetics and thermal stability of molecular hydrogen stored in a $B_{36}N_{36}$ cage. We find that hydrogen atoms prefer to remain inside the cage in molecular form and up to 18 H_2 molecules can be trapped at zero temperature. This amounts to a gravimetric density of 4 wt %, which is much larger than what has been possible in carbon-based nanostructures or has been seen for BN nanotubes. Unfortunately, the energy cost to store this amount of hydrogen is high and the storage material is not suitable for practical applications, as hydrogen is found to escape from the cage at room temperature.

Acknowledgment. The work was supported in part by a grant from the Department of Energy (DEFG02-96ER45579). The authors thank the crew of the Center for Computational Materials Science, the Institute for Materials Research, and Tohoku University, Japan for their continuous support of the HITAC SR8000 supercomputing facility. Q.S. thanks Dr. Maciej Gutowski in Pacific Northwest National Laboratory for useful discussions.

References

(1) Alper, J. *Science* **2003**, *299*, 1686.
(2) Cortright, R. D.; Davada, R. R.; Dumesic, J. A. *Nature* **2002**, *418*, 964.
(3) Chen, P.; Xiang, Z.; Luo, J. Z.; Tan, K. L. *Nature* **2002**, *420*, 302.
(4) Rosi, N. L.; Eckert, J.; Eddaoudi, M.; Vodak, D. T.; Kim, J.; O'Keefe, M.; Yaghi, O. M. *Science* **2003**, *300*, 1127.
(5) Schlappbach, L.; Zuttel, A. *Nature* **2001**, *414*, 353.
(6) See: http://www.sc.doe.gov/bes Basic_Research_Needs_To_Assure_A_Secure_Energy_Future_FEB2003.pdf.
(7) See http://www.sc.doe.gov/bes/hydrogen.pdf.
(8) Dillion, A. C.; Jones, K. M.; Bekkedahl, T. A.; Kiang, C. H.; Bethune, D. S.; Heben, M. J. *Nature* **1997**, *386*, 377. Chambers, A.; Park, C.; Baker, R. T. K.; Rodriguez, N. M. *J. Phys. Chem. B* **1998**, *102*, 4253.
(9) Liu, C.; Fan, Y. Y.; Liu, M.; Cong, H. T.; Cheng, H. M.; Dresselhaus, M. S. *Science* **1999**, *286*, 1127.
(10) Cheng, H. M.; Yang, Q. H.; Liu, C. *Carbon* **2001**, *39*, 1447.
(11) Darkrim, F. L.; Malbrunot, P.; Tartaglia, G. P. *Int. J. Hydrogen Energy* **2002**, *27*, 193.
(12) Zuttel, A.; Sudan, P.; Mauron, Ph.; Kiyobayashi, T.; Emmenegger, Ch.; Schlapbach, L. *Int. J. Hydrogen Energy* **2002**, *27*, 203.
(13) Dillon, A. C.; Gilbert, K. E.; Alleman, J. L.; Gennett, T.; Jones, K. M.; Parilla, P. A.; Heben, M. J. In Proceedings of the DOE Hydrogen Program Review, U. S.; 2001 (http:/www.eren.doe.gov/hydrogen/pdfs/30535am.pdf).
(14) Tibbetts, G. G.; Meisner, C. P.; OLK, C. H. *Carbon* **2001**, *39*, 2291.
(15) Shiraishi, M.; Takenobu, T.; Ata, M. *Chem. Phys. Lett.* **2003**, *367*, 633.
(16) Kajiura, H.; Tsutsui, S.; Kadono, K.; Kakuta, M.; Ata, M.; Murakami, Y. *Appl. Phys. Lett.* **2003**, *82*, 1105.
(17) Dodziuk, H.; Dolgonos, G. *Chem. Phys. Lett*. **2002**, *356*, 79.
(18) Blasé, X.; Rubio, A.; Louie, S. G.; Cohen, M. L. *Europhys. Lett.* **1994**, *28*, 335.
(19) Chopra, N. G.; Luyken, R. J.; Cherry, K.; Crespi, V. H.; Cohen, M. L.; Louie, S. G.; Zettl, A. *Science* **1995**, *69*, 966.
(20) Loiseau, A.; Williaime, F.; Demoncy, N.; Hug, G.; Pascard, H. *Phys. Rev. Lett.* **1996**, *76*, 4737.
(21) Han, W.; Bando, Y.; Kurashima, K.; Sato, T. *Appl. Phys. Lett*. **1998**, *73*, 3085.
(22) Lourie, O. R.; Jones, C. R.; Bartlett, B. M.; Gibbons, P. C.; Ruoff, R. S.; Buhro, W. E. *Chem. Mater*. **2000**, *12*, 1808.
(23) Chopra, N. G.; Zettl, A. *Solid State Commun*. **1995**, *105*, 297.
(24) Shrivastava, D.; Menon, M.; Cho, K. *Phys. Rev*. **2001**, *B63*, 195413.
(25) Tang, C.; Bando, Y.; Ding, X.; Qi, S.; Goldberg, D. *J. Am. Chem. Soc*. **2002**, *124*, 14550.
(26) Ma, R.; Bando, Y.; Zhu, H.; Sato, T.; Xun, C.; Wu, D. *J. Am. Chem. Soc*. **2002**, 124, 7672.
(27) Oku, T.; Naritab, I.; Nishiwakic, A.; Koid, N. *Defect Diffusion Forum* **2004**, *226−228*, 113.
(28) Oku, T.; Kuno, M.; Narita, I. *J. Phys. Chem. Solids* **2004**, *65*, 549.
(29) Oku, T.; Narita, I. *Physica B* **2002**, *323*, 216.
(30) Narita, I.; Oku, T. *Diamond Relat. Mater*. **2002**, 11,945.
(31) Bloechl, P. E. *Phys. Rev. B* **1994**, *50*, 17953.
(32) Kresse, G.; Heffner, J. *Phys. Rev. B* **1996**, *54*, 11169.
(33) Wang, Y.; Perdew, J. P. *Phys. Rev. B* **1991**, *44*, 13298.
(34) *CRC Handbook of Chemistry and Physics*; Lide, D. R., Ed.; CRC Press: New York, 2000.
(35) Alexandre, S. S.; Chacham, H.; Nunes, R. W. *Appl. Phys. Lett*. **1999**, *75*, 61.
(36) Mills, G.; Jónsson, H.; Schenter, G. K. *Surf. Sci.* **1995**, *324*, 305.
(37) Rubin, Y.; Jarrosson, T.; Wang, G.; Bartberger, M. D.; Houk, K. N.; Schick, G.; Saunders, M.; Cross, R. J. *Angew. Chem., Int. Ed*. **2001**, *40*, 1543.
(38) Nose, S. *J. Chem. Phys.* **1984**, *81*, 511.

NL050385P